

Research Paper

Focal adhesion kinase inhibitors prevent osteoblast mineralization in part due to suppression of Akt-mediated stabilization of osterix



Scott A. Gunn^a, Lauren M. Kreps^{a,b}, Huijun Zhao^a, Katelyn Landon^{a,b}, Jacob S. Ilacqua^a, Christina L. Addison^{a,b,c,*}

^a Program for Cancer Therapeutics, Ottawa Hospital Research Institute, Ottawa, ON K1H 8L6, Canada

^b Department of Biochemistry Microbiology and Immunology, University of Ottawa, Ottawa, ON K1H 4M5, Canada

^c Department of Medicine, University of Ottawa, Ottawa, ON K1H 4M5, Canada

ARTICLE INFO

Keywords:

Focal adhesion kinase
Osteoblast
Bone mineralization
Akt
FAK TKI
Alkaline phosphatase
Osterix

ABSTRACT

Focal Adhesion Kinase (FAK) is an important regulator of tumor cell proliferation, survival and metastasis. As such it has become a therapeutic target of interest in cancer. Previous studies suggested that use of FAK tyrosine kinase inhibitors (TKIs) blocks osteolysis in *in vivo* models of bone metastasis. However, from these studies it was not clear whether FAK TKIs blocked bone degradation by osteoclasts or also promoted bone formation by osteoblasts. In this study we evaluated whether use of the FAK TKI PF-562,271 affected the differentiation of pre-osteoblasts, or activity of mature differentiated osteoblasts. MC3T3-E1 pre-osteoblastic cells were treated with various doses of PF-562,271 following 3 or 10 days of differentiation which led to the inhibition of alkaline phosphatase (ALP) expression and reduced viable cell numbers in a dose-dependent manner. MC3T3-E1 cells which had been differentiated for 21 days prior to treatment with PF-562,271 showed a dose dependent decrease in mineralization as assessed by Alizarin Red staining, with concomitant decreased expression of ALP which is known to facilitate the bone mineralization activity of osteoblasts, however mRNA levels of the transcription factors RUNX2 and osterix which are important for osteoblast maturation and mineralization appeared unaffected at this time point. We speculated that this may be due to altered function of RUNX2 protein due to inhibitory phosphorylation by GSK3 β . We found treatment with PF-562,271 resulted in increased GSK3 β activity as measured by reduced levels of phospho-Ser9-GSK3 β which would result in phosphorylation and inhibition of RUNX2. Treatment of 21 day differentiated MC3T3-E1 cells with PF-562,271 in combination with GSK3 β inhibitors partially restored mineralization however this was not statistically significant. As we observed that FAK TKI also resulted in suppression of Akt, which is known to alter osterix protein stability downstream of RUNX2, we examined protein levels by western blot and found a dose-dependent decrease in osterix in FAK TKI treated differentiated MC3T3-E1 cells which is likely responsible for the reduced mineralization observed. Taken together our results suggest that use of FAK TKIs as therapeutics in the bone metastatic setting may block new bone formation as an off-target effect and thereby exacerbate the defective bone regulation that is characteristic of the bone metastatic environment.

1. Introduction

Bone is the most common site of metastasis for breast cancer [1]. Normal bone formation is usually tightly controlled by the counteracting activities of osteoblasts which form new bone, and osteoclasts which degrade bone. However, once tumors establish in bone, they dysregulate

normal bone homeostasis to promote aberrant bone degradation or excessive bone formation, with both processes ultimately leading to bone weakening. For osteolytic inducing tumors, bone osteolysis may be due in part to their ability to inhibit osteoblast differentiation or activity thereby reducing bone formation, and/or by increasing osteoclast differentiation or activity to promote bone degradation. Tumor-induced

Abbreviations: ALP, alkaline phosphatase; As, antisense; AAB, ascorbic acid and β -glycerophosphate; BGP, β -glycerophosphate; BSA, bovine serum albumin; DTT, 5-bromo-4-chloro-3-indolyl- β -D-galactopyranoside dithiothreitol; FAK, focal adhesion kinase; SA, senescence associated; TG, Tideglusib; TKI, tyrosine kinase inhibitor.

* Corresponding author at: Box 926, 501 Smyth Road, Ottawa, ON K1H 8L6, Canada.

E-mail address: caddison@ohri.ca (C.L. Addison).

<https://doi.org/10.1016/j.jbo.2022.100432>

Received 29 September 2021; Received in revised form 6 April 2022; Accepted 19 April 2022

Available online 13 May 2022

2212-1374/© 2022 Published by Elsevier GmbH. This is an open access article under the CC BY-NC-ND license (<http://creativecommons.org/licenses/by-nc-nd/4.0/>).

osteolysis leads to what is termed the ‘vicious cycle’ [2], where tumor produced factors inhibit osteoblast activity and promote osteoclast activity leading to bone degradation. In turn, this degradation of the bone matrix results in the release of growth factors that stimulate tumor cell proliferation leading to further induction of bone degradation. Since bone destruction leads to many undesirable clinical problems such as risk of fracture and significant bone pain in metastatic patients, many treatments for bone metastatic malignancies are designed to block the process of osteolysis. These treatments however have not benefitted patients with respect to overall survival, hence new treatments are warranted.

Focal adhesion kinase (FAK) is a cytoplasmic tyrosine kinase which has been shown to promote tumor cell proliferation, survival and invasion [3,4]. FAK also regulates tumor progression and metastases in transgenic mouse models [5], and is correlated with higher tumor grades and metastasis [3,6–10]. In bone, FAK induces expression of RANKL [11], is important in recruitment and migration of osteoclast precursors [12], and is activated in mature osteoclasts [13,14] where it contributes to degradation of bone matrix [15,16]. As such it is potentially an important therapeutic target for cancer and many small molecule inhibitors which block its activity have been developed in recent years. Most FAK tyrosine kinase inhibitors (TKI), such as PF-562,271 are small molecule ATP mimetics that affect the ability of FAK to function as a kinase [17,18] but may not affect its ability to act as a scaffolding protein which has also been shown to be important in tumor progression [19–21]. In mouse models of bone metastasis, treatment with FAK inhibitors has been previously shown to inhibit osteolysis in tumor-bearing bones [22–24]. However, these studies did not determine whether the activity of FAK TKIs in vivo only prevented further bone destruction or were also able to restore osteoblast differentiation and bone formation activity.

To assess the role of FAK in osteoblast differentiation, Kim et al. [14] generated collagen type I(α)I promoter driven-Cre expression to generate FAK-null osteoblasts in FAK^{fl/fl} mice and found that FAK mutant embryos had an intact skeleton suggesting FAK was either dispensable for osteoblast differentiation, or its absence was compensated for by alternative factors in this process during embryogenesis. However, they found that FAK^{-/-} (p53^{-/-}) calvarial derived osteoblasts from adult mice showed delayed bone formation in response to injury, with a decrease in alkaline phosphatase (ALP) activity. In MC3T3 cells, ALP activity was shown to be reduced in cells transfected with antisense FAK (asFAK) [25], and its depletion using this approach was also shown to inhibit BMP-2 induced ALP activity, osteocalcin expression and mineralized nodule formation [26]. These data support a role for FAK in osteoblast differentiation and bone formation in adults, and as such, the use of therapeutic strategies to block FAK activity in vivo in the context of bone metastatic cancers, could lead to detrimental effects on bone regeneration in patients. Thus, we further investigated the impact of FAK inhibition using specific TKIs on the ability of pre-osteoblasts to differentiate and induce bone mineralization and attempted to ascertain important signaling activities associated with the observed phenotypes following treatment with FAK TKIs.

2. Methods and materials

2.1. Cell lines and reagents

Mouse calvarial MC3T3-E1 subclone 4 (CRL-2593) pre-osteoblast cells were obtained from ATCC. MC3T3-E1 cells were routinely maintained in Alpha Modified Eagle’s Medium (αMEM) containing 10 % FBS (Hyclone, ThermoFisher Scientific, Ottawa ON), and 1 mM sodium pyruvate (11360-070, Gibco, ThermoFisher Scientific, Ottawa ON) and incubated at 37 °C with 5 % CO₂. Osteoblast differentiation reagents L-ascorbic acid (A4403) and β-glycerophosphate (BGP) disodium salt hydrate (G9422) were obtained from Sigma-Aldrich (Oakville, ON). Leukocyte alkaline phosphatase 86R staining kit was also obtained from

Sigma-Aldrich (Oakville, ON). The following antibodies were obtained from Cell Signaling (Danvers MA, USA): Phospho-Akt (Ser473), total AKT, phospho-FAK (Tyr397), p53, phospho-Ser9/21 GSK3β, total GSK3β, phospho-ERK1/2, phospho-p38, total p38 and cleaved caspase-3. Osterix and GAPDH antibodies were obtained from Abcam (Toronto, ON), while total ERK1/2 antibodies were from Santa Cruz Biotechnology (Dallas TX, USA) and β-actin antibodies from Sigma (Oakville ON). Shh, Wnt3a and BMP2 antibodies were from R&D Systems (Minneapolis, MN, USA). Total FAK antibodies were from BD Transduction Laboratories (BD Biosciences, San Jose CA, USA). All primary antibodies were used at a 1:1000 dilution. Goat anti-mouse and goat anti-rabbit secondary antibodies were from Jackson ImmunoResearch (West Grove PA, USA) and were used at a dilution of 1:5000. All inhibitors used in this study were from Selleckchem distributed by Cedarlane (Burlington ON) with the exceptions of SP141 and PF-573,228 which were from Tocris-BioTechnique (Toronto ON) and PF-562,271 which was from Cayman Chemical distributed by Cedarlane (Burlington ON).

2.2. Osteoblast differentiation, cell viability and ALP staining

For differentiation into osteoblasts, MC3T3-E1 cells were seeded at 5×10^4 cells/well in 6-well plates, and the next day stimulated with αMEM supplemented with 1 mM sodium pyruvate, 10 % fetal bovine serum, 0.3 mM ascorbic acid, and 10 mM BGP differentiation media. Differentiation media was changed every 2–3 days for 7–21 days. The number of viable cells following PF-562,271 administration was determined at 7 days (3 days differentiation with drug addition for 4 days thereafter) and at 14 days (10 days differentiation with drug addition for 4 days thereafter) by trypsinizing cells and counting viable cell numbers per well using trypan blue exclusion detection in the ViaXR Cell Counter. For studies assessing ALP expression early during MC3T3-E1 differentiation PF-562,271 was added 4 days prior to ALP staining. For ALP staining, cells were fixed using a mixture of formaldehyde, acetone and citrate for 30 s. Cells were washed, and then stained using the Sigma ALP stain kit according to the manufacturer’s directions. Cells were counterstained using hematoxylin. ALP was quantified using Image J with thresholding to detect ALP stain and determination of the percentage area that was ALP positive in three random fields of view in each of 5 randomly taken images per well. To determine the percentage of ALP positive cells, the cell counter mode in Image J was used to identify 200 randomly chosen cells in three random fields of view in each of three randomly taken photos per well, and of these 200 identified cells, the number that were ALP positive was counted in a second channel to calculate percent ALP positive cells per well.

2.3. Assessment of osteoblast mineralization

For assessing mineralization in differentiated MC3T3-E1 cells, various concentrations of drugs were added on day 21–22, and differentiation media containing drugs replaced every 2–3 days for an additional 7–8 days. For Alizarin red staining, on day 28–29 media was removed and cells washed once with PBS prior to fixation with ice cold 70 % ethanol for 1 h at room temperature. Cells were then washed 3x with ddH₂O and 1 mL of Alizarin red stain (Millipore, Etobicoke ON) was added and cells incubated at room temperature for 20mins with gentle rocking. Cells were washed 4x with ddH₂O, and 3 images were taken per well under a dissecting microscope and ImageJ was then used to quantify the mineralized area in each image. After imaging, the dye was extracted by adding 800uL of 10 % acetic acid to each well and incubating at room temperature for 30mins on a rocker. Cells were then scraped into a 1.5 mL centrifuge tube with the acetic acid and vortexed for 30 s, followed by heating at 85 °C for 10mins, and centrifugation at 20,000×g for 20mins. Supernatant was then transferred to a new tube and 200uL of 10 % ammonium hydroxide was added. A 150uL aliquot of each sample was then loaded in duplicate wells in a 96-well plate and the absorbance was read at 405 nm in a Multiskan plate reader

(ThermoFisher Scientific, Ottawa ON).

2.4. Western blot analysis

Protein was collected from cells for analysis by western blot by lysis in radioimmunoprecipitation assay (RIPA) buffer containing 1x protease inhibitor cocktail (2 mM 4-(2-Aminoethyl) benzenesulfonyl fluoride hydrochloride (AEBSF), 0.3 μ M Aprotinin, 116 μ M Bestatin, 14 μ M E-64, 1 μ M Leupeptin, 1 mM EDTA; Sigma-Aldrich, Oakville, ON). The lysis buffer and cells were collected and frozen at -80°C to further lyse the cells. After a freeze/thaw cycle, the samples were centrifuged for 5 mins at $14,000\times g$ at 4°C , the supernatant was then collected and either frozen at -80°C or immediately quantified using the Bio-Rad Protein Assay Dye Reagent Concentrate (Bio-Rad, Mississauga, ON), and absorbance measured at 595 nm using the BioMate 3 (Thermo Fisher Scientific, Ottawa ON) to provide a protein concentration in mg/mL after performing interpolation of a standard curve generated from known quantities of bovine serum albumin (BSA). A total of 50 μ g of protein was subjected to denaturation by addition of 1X β -mercaptoethanol based sample loading buffer followed by incubation at 100°C for 5 min to denature proteins. Samples were then subjected to electrophoresis in 10 % Tris-polyacrylamide gels in glycine based running buffer at 140 V in the BioRad western apparatus system, with inclusion of a BLUeye Prestained Protein Ladder (FroggaBio Inc, Toronto, ON) to facilitate identification of protein molecular weights. Proteins were then transferred to Immobilon-P PVDF membrane (Millipore Ltd., Etobicoke, ON) by electrophoresis, and non-specific sites on the membrane were blocked in 5 % blocking solution consisting of either skim milk or bovine serum albumin (BSA) in 1X TBST (TBS with 1 % Tween-20) for approximately 1 h at 4°C on a platform rocker. Membranes were then incubated with specific primary antibody diluted in either 5 % skim milk or 5 % BSA in 1X TBST and incubated overnight at 4°C on a platform rocker, followed by washing three times with 1X TBST for approximately 5 min each. Membranes were then incubated with appropriately diluted secondary antibody for 1 h at room temperature followed by 5 washes with 1X TBST. Protein antibody conjugates were then visualized following addition of Bio-Rad Clarity Western ECL Substrate (Bio-Rad, Mississauga, ON) and subsequently imaged using either the Genegnome Syngene Bio Imaging imager (Syngene, Frederick, MD) or HyBlot CL Autoradiography Film (Denville Inc., Saint-Laurent, QC) and JP33 JPI Automatic X-ray film processor (JPI Healthcare, Plainview, NY).

2.5. RNA extraction, cDNA synthesis and qRT-PCR

RNA was extracted from cells using the RNeasy kit (Qiagen, Montreal, QC), quantified following measurement of absorbance at 260 nm on a spectrophotometer and stored at -80°C . Complementary DNA (cDNA) was synthesized by combining 1 μ g of total RNA with 10 mM dNTP, and Oligo (dT) (Invitrogen, ThermoFisher, Ottawa ON) to prime the reaction. The sample was then heated at 65°C for 5 min. A total of 4 μ L of 5x First Strand Buffer, 1 μ L of RNase out, and 2 μ L of 0.1 M dithiothreitol (DTT) were then added to each tube, and the samples were heated at 37°C for 2 min. Subsequently, 1 μ L of Moloney murine leukemia virus (M-MLV) reverse transcriptase (Invitrogen, ThermoFisher, Ottawa ON) was then added to each sample. The samples were then incubated at 37°C for 50 min, followed by inactivation at 70°C for 15 min. cDNA was stored at -20°C until further use.

Polymerase chain reaction (PCR) was performed using cDNA, individual primers (forward and reverse) for specific genes of interest, nuclease free water and RT SYBR Green ROX qPCR Mastermix (Qiagen, Montreal, QC), using the 7500 Fast Real-Time PCR System (Applied Biosystems by life Technologies, Carlsbad, CA). The reaction was completed with the following steps, denaturation at 95°C for 10 min, followed by PCR for 40 cycles, using denaturation of 95°C for 15 sec and elongation at 60°C for 1 min. The following primers were used: Osterix (forward AGCGACCACTTGAGCAAACAT, reverse GCGGCTGATT

GGCTTCTCT), BMP2 (forward GGGACCCGCTGTCTCTAGT, reverse TCAACTCAAATTCGCTGAGGAC), Shh (forward AAAGCTGACCCCTT-TAGCCTA, reverse TTCGGAGTTTCTTGTGATCTTCC), Wnt3a (forward CTGGCAGCTGTGAAGTGAAG, reverse TGGGTGAGGCCTCGTAGTAG), RUNX2 (forward ATTCAGGGGAACCCAAAAAG, reverse, GCGACTT-CATTTCGACTTCTCT), OPG (forward ACCCAGAAACTGGTCATCAGC, reverse CTGCAATACACACTCATCACT), osteocalcin (forward 5-GCAATAAGGTAGTGAACAGACTCC-3, reverse, 5-GTTTGTAGGCGGTC TCAAGC-3; and β -actin (forward CTAAGGCCAACCGTGAAAAG, reverse ACCAGAGGCATACAGGGACA).

2.6. SA- β -galactosidase staining

Differentiated MC3T3-E1 cells were treated with FAK inhibitor for 7 days, and cells were fixed and stained for expression of senescence associated (SA) β -galactosidase essentially as described [27]. Briefly, cells were washed twice with PBS, then fixed with a formaldehyde/glutaraldehyde solution for 15 min at room temperature. Cells were washed again twice with PBS prior to addition of X-gal staining solution (40 mM citric acid/Na phosphate buffer, 5 mM K₄ [Fe(CN)₆] 3H₂O, 5 mM K₃ [Fe(CN)₆], 150 mM NaCl, 2 mM MgCl and 1 mg/ml 5-bromo-4-chloro-3-indolyl- β -D-galactopyranoside) and incubation overnight at 37°C . Cells were subsequently imaged under brightfield at 100X using the Nikon Eclipse TE2000-U (Nikon, Mississauga, ON) microscope.

2.7. Statistical analysis

Statistical analysis was performed using Graph Pad Prism 5 software. Experiments comparing two groups were compared using a student's *t*-test. Experiments comparing more than two groups were compared using a one-way ANOVA with a Bonferroni post-test. P-values were considered significant at <0.05 (* $p < 0.05$, ** $p < 0.01$, *** $p < 0.001$).

3. Results

3.1. Effect of FAK TKIs on MC3T3-E1 osteoblast differentiation.

As use of FAK inhibitors to block progression of bone metastatic cancers may be an effective therapeutic approach, we wanted to investigate the potential effects of these agents on other cells in the bone metastatic tumor microenvironment. As there is some precedent that FAK is necessary for bone formation in response to injury in adults, we initially investigated the effects of the FAK TKI PF-562,271 on the ability of the model pre-osteoblast cell line, MC3T3-E1, to differentiate into mature osteoblasts. MC3T3-E1 were thus treated with ascorbic acid and β -glycerophosphate (AAB) to induce differentiation into osteoblasts, and following 4 days (early), or 10 days (late) of AAB treatment, previously established efficacious dose ranges of PF-562,271 [17,28,29] or DMSO as a vehicle control was added to differentiation media. Expression of ALP was assessed 3–4 days post initiation of drug treatment. We observed that ALP expression was reduced dose-dependently following addition of PF-562,271 both at early and late times during the differentiation process (Fig. 1A). Quantification of ALP expression showed dose-dependent decreases in ALP staining (Fig. 1B for D7 and Supplementary Fig. S1A for D14) and the percentage of ALP+ cells (Fig. 1C). We tested the viability of differentiating MC3T3-E1 cells following PF-562,271 treatment by direct counting of trypan blue excluding cells and observed dose-dependent decreases in cell viability at both D7 (Fig. 1D) and D14 (Supplementary Fig.S1B). We tested whether the reduced cell viability could be due to apoptosis by measuring levels of cleaved PARP and cleaved caspase-3, however did not observe any significant increases in either of these apoptotic markers in PF-562,271 treated cells (Fig. 1E). Additionally, in long term differentiation assays whereby addition of PF-562,271 was given after 21 days of AAB-induced differentiation, when cells begin to mineralize, PF-562,271 dose-dependently inhibited osteoblast mineralization, as detected by Alizarin

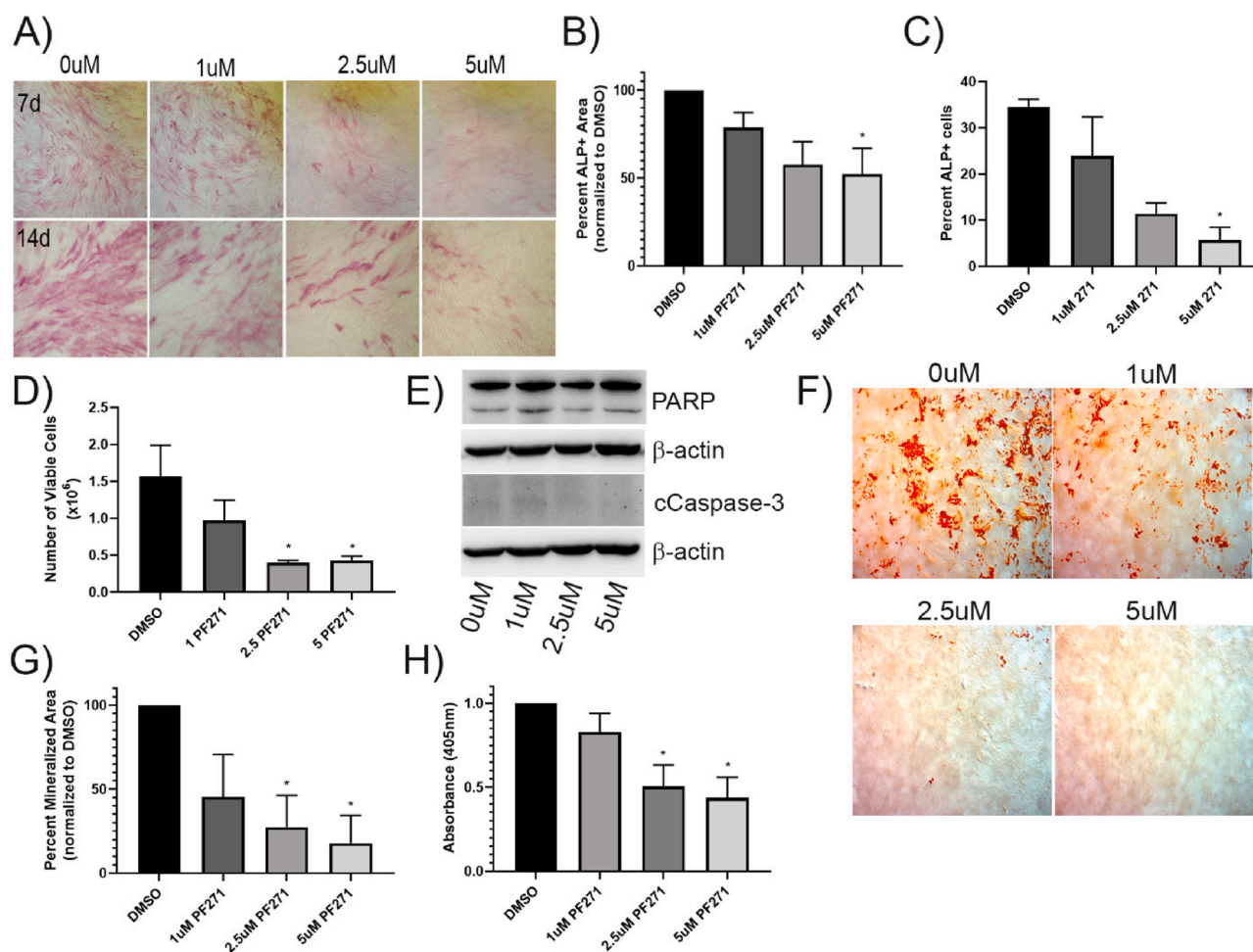


Fig. 1. PF-562,271 treatment inhibits ALP expression and mineralization in MC3T3-E1 cells induced to undergo osteoblast differentiation. (A) MC3T3-E1 cells were plated and the next day (D1) growth media was replaced with media containing β -glycerophosphate and ascorbic acid, followed by addition of various concentrations of PF-562,271 or DMSO as a vehicle control starting on D4 or D10. Levels of expression of ALP were assessed as described in the Methods on D7 (top panel) or D14 (bottom panel) post differentiation and were imaged for comparison. (B) ALP staining was quantified using image J analysis as described in the Methods in five randomly chosen images for each of duplicate wells in three independent biological replicates. (C) The percentage of ALP + cells from (A) were also determined using Image J assisted quantification in a minimum of 200 cells in three randomly chosen fields of view in each of triplicate images taken from duplicate wells in each independent experiment ($n = 3$). (D) MC3T3-E1 cells were differentiated and treated with drug as described in (A) and at D7 were harvested and viable cell number per well enumerated using trypan blue exclusion and counting on the ViaXR Cell Counter. Cells were counted in duplicate wells for each of 3 independent biological replicates. (E) Western blot analysis of cells treated as in (A) for apoptotic markers cleaved PARP and cleaved caspase-3 with β -actin as a loading control. (F) MC3T3-E1 cells were plated and induced to differentiate as described in (A), and 21 days later various concentrations of PF-562,271 were added to differentiation media. Seven days later (28 days post initiation of differentiation), cells were assessed for mineralization using Alizarin red staining as described in the Methods section with representative images from each condition shown. (G) Alizarin red staining in 5 random fields of view in duplicate wells for each of three independently performed biological replicates was quantified in representative images using image J as described in the Methods. (H) Following imaging, dye in each well was extracted and the absorbance measured as described in the Methods. Graphs represent the mean and standard error of duplicate wells from each of three independent biological replicates with * representing p -value < 0.05 ; ** representing p -value < 0.01 .

red staining (Fig. 1F, quantified by ImageJ analysis (Fig. 1G) and measurement of levels of extracted stain from cells (Fig. 1H)). As PF-562,271 is also known to inhibit the FAK family member Pyk2 at 8-fold higher doses, and Pyk2 has been implicated in osteoblastogenesis [30,31], we also tested the effects of the FAK TKI PF-573,228, which is more selective for FAK inhibition and only affects Pyk2 activity at 250-fold higher concentrations, on the ability of MC3T3-E1 cells to mineralize. We found that similar to PF-562,271, PF-573,228 also impaired mineralization in a dose-dependent manner (Fig. 2A&B).

We next investigated the effects of PF-562,271 on various factors known to be associated with osteoblast differentiation and mineralization. For two important transcriptional mediators of osteoblastogenesis and bone mineralization, we saw no significant changes in the mRNA expression levels of osterix but observed increased Runx2 expression at the highest dose of PF-562,271 (Fig. 3A&B). We also observed

significant increases in the expression level of factors associated with osteoblastogenesis such as Wnt3a, BMP-2 and Shh (Fig. 3C-E) with addition of higher doses of PF-562,271. These observed patterns of expression at the mRNA level suggest that osteoblastogenesis and bone mineralization should be enhanced. However, as this was opposite to what we observed, we attempted to confirm elevated cellular protein levels of these factors. We were unable to reliably detect levels of BMP-2 or Shh (could not detect any BMP2 and Shh levels were very low (Fig. 3F)) in cell lysates possibly due to the fact that these are secreted proteins. We also did not observe parallel increases in cellular Runx2 protein (see Fig. 6A) nor in the soluble factor Wnt3a (Fig. 3F) in protein lysates isolated after PF-562,271 treatment of 21-day differentiated MC3T3-E1 cells.

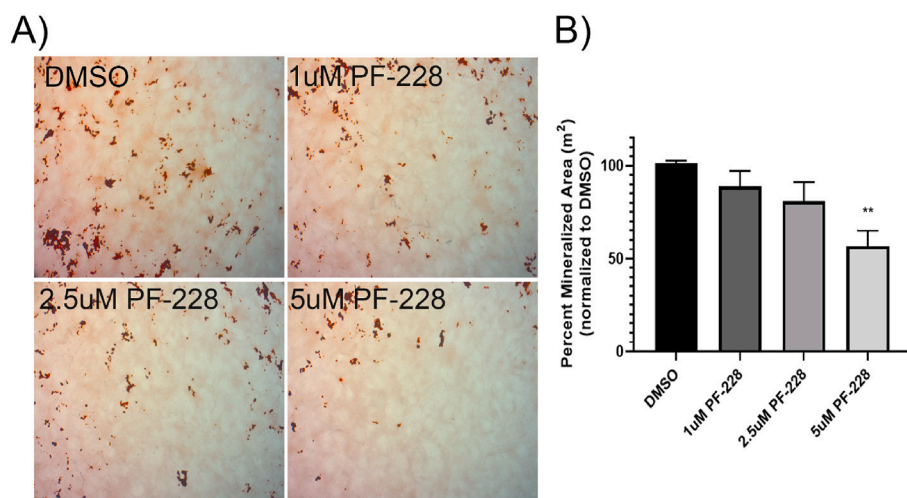


Fig. 2. The selective FAK inhibitor PF-573,228 inhibits osteoblast mineralization. MC3T3-E1 cells were plated and induced to differentiate as described in the Methods, and 21 days post-initiation of differentiation various concentrations of the selective FAK inhibitor PF-573,228 or DMSO as a vehicle control were added. Mineralization was then assessed on D28 by Alizarin red staining and wells were imaged and the percentage of Alizarin red stain quantified using Image J as described in the Methods. Representative images are shown in (A), while Alizarin red stain quantification is shown in (B) and expressed as the mean with associated standard error for duplicate wells in each of three independent biological experiments. ** p-value < 0.01.

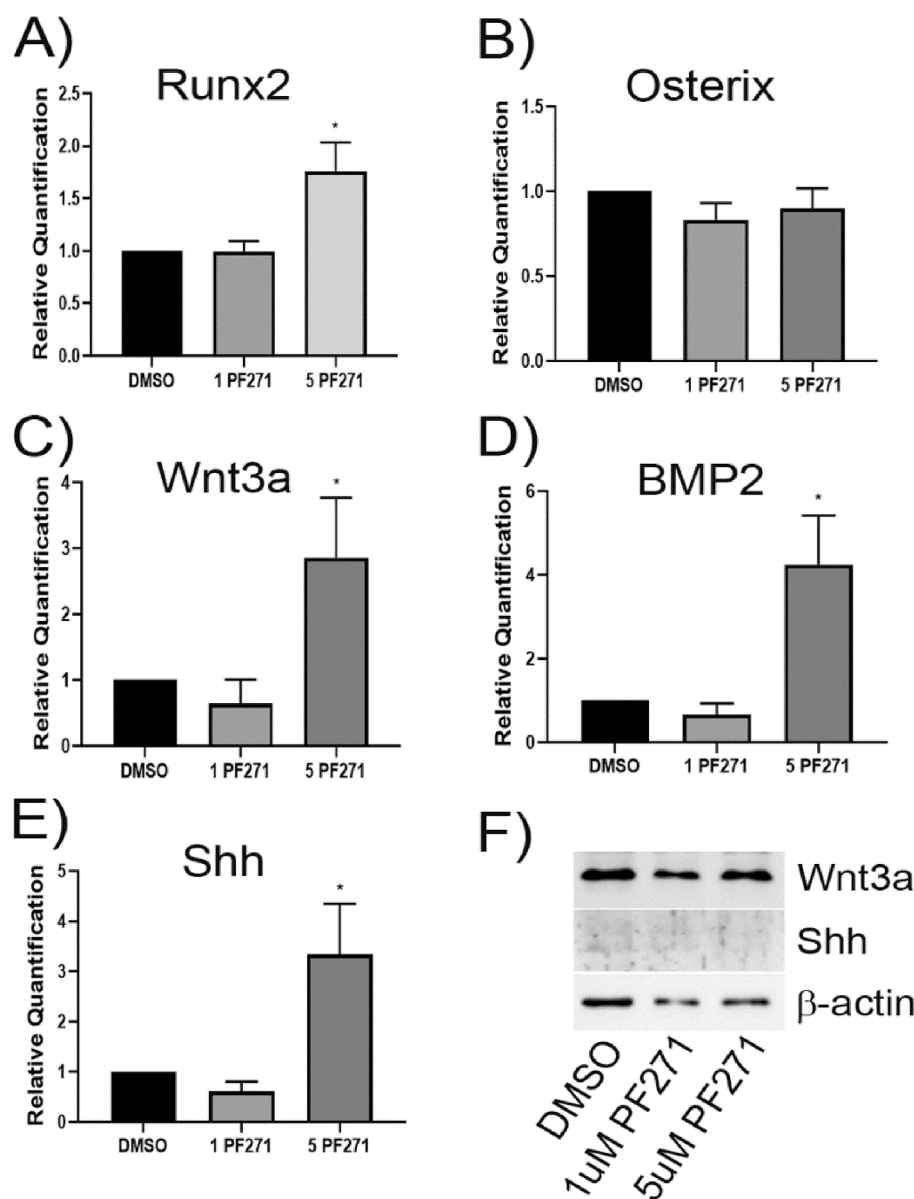


Fig. 3. Treatment of 21-day differentiated MC3T3-E1 cells with PF-562,271 results in alterations in expression of Wnt, BMP2 and Shh but has no effect on Runx2 or Osterix mRNA levels. MC3T3-E1 cells were differentiated with ascorbic acid and β-glycerophosphate for 21 days as described in the Methods. Cells were then treated for 96 h with DMSO or various concentrations of PF-562,271, replacing the media containing drug every 2 days. At D7 post initiation of drug treatment RNA was collected, and qRT-PCR performed using murine specific primers to assess the expression of A) RUNX2, B) Osterix, C) Wnt3a, D) BMP2, or E) Shh. Graphs represent the mean relative expression normalized to β-actin levels and DMSO as a control condition for triplicate technical replicates in n = 3 independent biological replicates. * p < 0.05, ** p < 0.01. (F) Cellular protein lysates were also generated at D28 (following initiation of PF-562,271 treatment at D21 of MC3T3-E1 differentiation) and assessed for levels of Wnt3a or Shh by western blot analysis with β-actin used as a control for total protein loading.

3.2. FAK TKI-mediated suppression of differentiated MC3T3-E1 mineralization is not reversed by inhibition of BMP or Wnt pathways.

Although we did not observe significant increases in protein expression of Wnt3a and BMP-2, we were concerned that since these are secreted proteins this could affect the reliable detection of their altered levels in cellular protein lysates. Thus, we decided to test whether they played a role in the lack of mineralization by differentiated MC3T3-E1 cells following PF-562,271 treatment. BMP and Wnt both participate in osteoblast differentiation, however, the timing of these signals is critical. It has been suggested that when Wnt signaling is activated in the presence of BMP-2, Wnt3a down-regulates osteoblast differentiation through a p53-associated pathway resulting in the decreased expression of Osterix and ALP [32]. While we did not see any difference in osterix expression levels, we did see a decrease in ALP in 14 day differentiated drug treated MC3T3-E1 cells (Fig. 1A) suggesting this could play a role at later time points. To test the hypothesis that FAK inhibitor treatment reduced mineralization due to inappropriately altered BMP and Wnt signaling, MC3T3-E1 cells were differentiated for 21 days and then treated with a BMP inhibitor (LDN193189) or a Wnt inhibitor (XAV939 or Wnt C59) alone or in combination with PF-562,271 and mineralization was assessed. LDN193189 inhibits BMP signals by blocking the activation of the intracellular SMAD proteins (SMAD1, 5, and 8) which are responsible for transducing the extracellular BMP signal into an intracellular signal. Addition of LDN193189 as a single agent resulted in decreased levels of phospho-SMAD1 (Fig. 4B) and decreased mineralization as expected (Fig. 4A). However, when combined with PF-562,271, inhibition of BMP signaling by LDN193189 did not rescue the impaired mineralization observed following treatment with the FAK TKI (Fig. 4A). XAV939 inhibits Wnt signaling by stimulating the degradation of the downstream signal transducer β -catenin, thereby blocking its nuclear signaling functions. Although reduced levels of β -catenin (Fig. 4B) were observed when XAV939 was used in combination with PF-562,271 there was no significant change in mineralization which remained impaired (Fig. 4A). Lastly, Wnt C59 blocks the acetylation of Wnt proteins which in turn blocks their activity. Although Wnt C59 showed a decrease in mineralization when used alone, no ability to rescue mineralization when combined with PF-562,271 was observed (Fig. 4A). As both BMP and Wnt signals are required mainly for osteoblast differentiation, and in our long-term assay system, osteoblasts have already been differentiated for 21 days and are ready to mineralize prior to drug addition, it is possible that FAK inhibition is blocking additional pathways which are specifically more functional at the mineralization stage. It is also possible that the upregulation of Wnt3a and BMP2 mRNA following treatment with PF-562,271 does not result in increased levels of their respective proteins as we were unable to show significant upregulation following their assessment by western blot

analysis (Fig. 3F).

To assess whether FAK inhibition could alter these pathways at earlier time points, which could ultimately affect MC3T3-E1 cell differentiation, we also examined expression of a number of targets by qRT-PCR at day 7 (3 days differentiation with drug treatment starting on D4) or day 14 (9 days differentiation with drug treatment starting on D10). We saw similar trends with dose-dependent increases in expression of Wnt3a, BMP-2 and Shh at day 7 with similar increases at lower doses of PF-562,271 observed at the 14-day time point. Interestingly, despite observing no change in osterix and an increase in Runx2 expression in D28 (ie 21 day differentiated cells with drug treatment for an additional 7 days), treatment of shorter term differentiated MC3T3-E1 cells showed statistically significant decreases in Runx2 and osterix mRNA levels at both the D7 and D14 time points (Supplementary Fig.S2), which could in part explain the reduced levels of ALP expression observed at these early time points (Fig. 1A).

3.3. Inhibition of Mdm2-mediated p53 degradation induced by FAK TKI does not restore mineralization.

Despite observing decreases in transcription factors important for osteoblastogenesis at early time points, we did not observe similar decreases when drug treatment was initiated at later time points when cells are already fully differentiated and starting to mineralize. As such, we looked for alternative pathways known to regulate osteoblastogenesis and mineralization that could be affected by FAK inhibitor treatment. Another important regulator of osteoblastogenesis is Mdm2 via its ability to suppress p53 and stabilize Runx2 expression [33]. As it has been previously shown that PF-562,271 can promote nuclear accumulation of FAK, and nuclear FAK can function to stabilize Mdm2 leading to increased p53 degradation [34], we hypothesized that perhaps PF-562,271 led to increased Mdm2 levels and alteration of homeostatic levels of its various targets resulting in impaired mineralization by treated osteoblasts. In line with previously described findings, we observed increased MDM2 levels and a dose dependent decrease in p53 protein levels following treatment of differentiated MC3T3-E1 with PF-562,271 supporting the notion that FAK TKI treatment stabilizes Mdm2 (Fig. 5A, densitometric analysis of $n = 3$ western blots shown in Supplementary Table S1). However, given the proposed role for p53 as an inhibitor of osteoblast differentiation [33], this finding would suggest FAK TKI treated MC3T3-E1 cells should have increased mineralization abilities which was not observed. As Mdm2 targets multiple proteins for ubiquitin-mediated proteasomal degradation, we speculated that FAK TKI treatment could be inducing degradation of other proteins required for osteoblast differentiation and mineralization, thus assessed whether addition of the proteasome inhibitor MG132 could restore mineralization. Although addition of MG132 inhibited the dose dependent

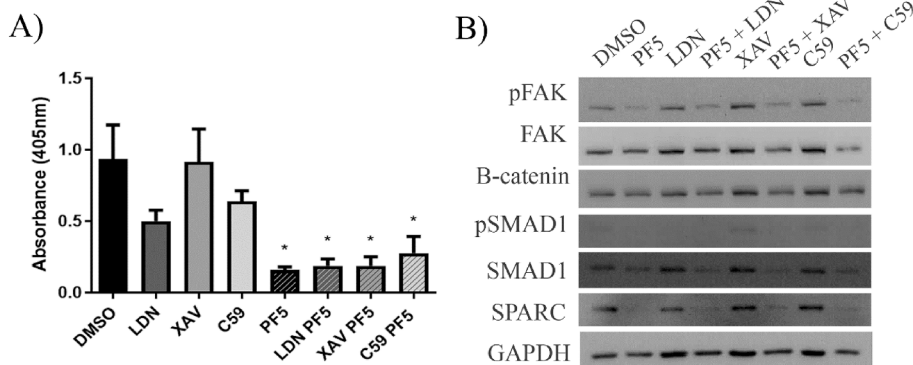


Fig. 4. Treatment of differentiated MC3T3-E1 cells with WNT or BMP inhibitors does not restore mineralization defects induced by PF-562,271. MC3T3-E1 cells were differentiated for 21 days as described in the Methods and were then treated with either DMSO as a vehicle control, 0.5uM LDN193189 (LDN), 1 nM Wnt-C59 (C59), or 5 nM XAV939 (XAV) alone or each in combination with 5uM PF-562,271 (PF5) for an additional 6 days. (A) On day 28, cells were stained with alizarin red and dye extracted and quantified as described in the Methods. Graphs represent the mean and standard error of duplicate wells in three independent biological replicates. (B) A set of replicate wells were used to generate protein extracts on day 27 which were subjected to western blot analysis to assess the levels of various proteins to ensure activity of the inhibitors administered. GAPDH assessment was included as a control to monitor equivalent protein loading.

tein loading.

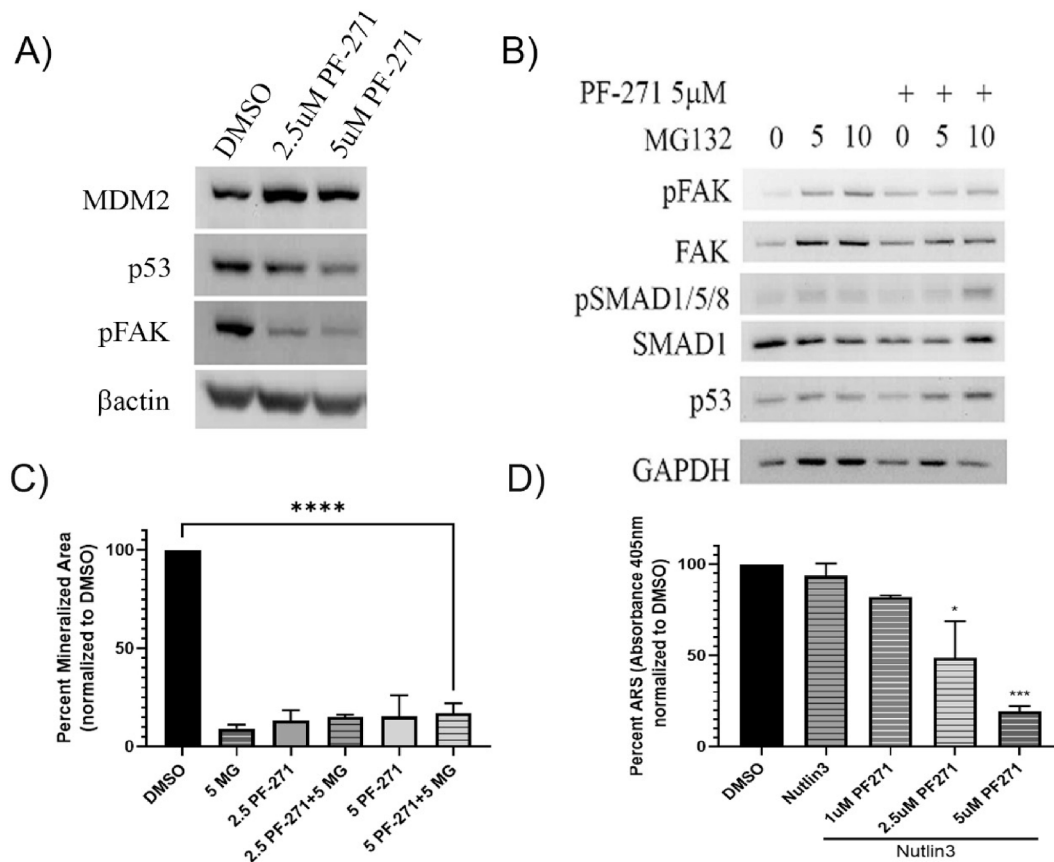


Fig. 5. Treatment of differentiated MC3T3-E1 cells with PF-562,271 increases Mdm2 stability leading to p53 depletion, however inhibition of proteasomal degradation or Mdm2 activity does not affect PF-562,271 mediated inhibition of mineralization. (A) MC3T3-E1 cells were differentiated for 21 days as described in the Methods and were then treated with either DMSO as a vehicle control or 2.5 μM or 5 μM of PF-562,271 (PF271) for an additional 6 days at which time protein lysates were generated. Samples were assessed for levels of various proteins including p53 as a marker of Mdm2 activity by western blot analysis. β-actin levels were assessed as a control for total protein loading. (B) 21 day differentiated MC3T3-E1 cells were treated with DMSO or 5 μM PF-562,271, and additionally treated with 0 μM, 5 μM or 10 μM MG132 proteasome inhibitor for an additional 6 days, at which time protein lysates were generated. Protein samples were subjected to western blot analysis for active FAK (phospho-Y397) as a control for effective suppression by PF-562,271, and phospho-SMAD1 and p53 levels as a control for effective proteasome inhibition by MG132. GAPDH was included as a control for equivalent protein loading. (C) 21 day differentiated MC3T3-E1 cells were treated with DMSO, 5 μM PF-562,271 (PF-271), or 5 μM MG132 (MG) proteasome inhibitor alone or in combination as indicated for an additional 6 days. Cells were then stained with alizarin red and stained areas quantified using image J as described in the Methods. Graphs represent the mean and standard error of alizarin red stained areas in duplicate wells in each of three independent biological replicates. (D) 21 day differentiated MC3T3-E1 cells were treated with DMSO or 10 μM nutlin3 (N3) alone or in the presence of increasing concentrations of PF-562,271, (PF271) for an additional 6 days at which time they were stained with alizarin red. Dye was extracted and absorbance measured as described in the Methods for quantification. Graphs represent mean and standard error of alizarin red absorbance extracted from duplicate wells in each of three independent biological replicates.

decrease in p53 following PF-562,271 treatment (Fig. 5B), it did not restore mineralization blocked by addition of PF-562,271 (Fig. 5C). As MG132 likely also alters levels of many other proteins given its function as a general proteome inhibitor, we further investigated this potential MDM2-p53 mechanism using a more specific MDM2 inhibitor, Nutlin-3, which blocks the MDM2-p53 interaction thereby inhibiting the degradation of p53. Similar to what we observed with use of MG132, addition of nutlin-3 did not change the dose-dependent inhibition of osteoblast mineralization induced by PF-562,271 which remained impaired (Fig. 5D).

3.4. FAK TKI treatment of differentiated MC3T3-E1 alters activity of cytoplasmic kinases, including activation of GSK3β.

Although our findings did not support a role for these pathways in restoring mineralization blocked by addition of PF-562,271, we consistently saw a decrease in ALP expression with FAK TKI treatment. This is in spite of the fact that we observed increases in BMP-2 and Shh (at least at the mRNA level) which have been reported to induce ALP expression [35]. As ALP is required for initiation of calcium deposition

during mineralization [36–38], we turned our attention to other factors regulating its expression as possible mediators of the mineralization impairment we observed following PF-562,271 treatment. One critical regulator of ALP expression is RUNX2. Although we initially saw no changes in RUNX2 mRNA levels at late time points (Fig. 2A), we confirmed that PF-562,271 treatment had no significant effect on total Runx2 protein levels (Fig. 6A, see Supplementary Table S3 for densitometry), including at early stages (i.e. addition after 4 days of differentiation induction), or at late stages of OB differentiation (i.e. addition after 21 days of differentiation). However, its ability to function as a transcription factor can also be regulated by phosphorylation events mediated by numerous cellular signaling proteins. One key regulating factor is ERK1/2 which has been shown to induce activation of Runx2 [39,40]. We tested the effects of PF-562,271 treatment on the activity of ERK1/2 by assessing its phosphorylation at T202/Y204 by western blot analysis. As can be seen in Fig. 6A, PF-562,271 induced activation of ERK1/2 (see Supplementary Table S3 for densitometry), which would suggest it should increase Runx2 activity and hence ALP expression. In a similar manner, p38 has also been shown to phosphorylate and increase the transcriptional activity of Runx2 [39,40]. We found that PF-562,271

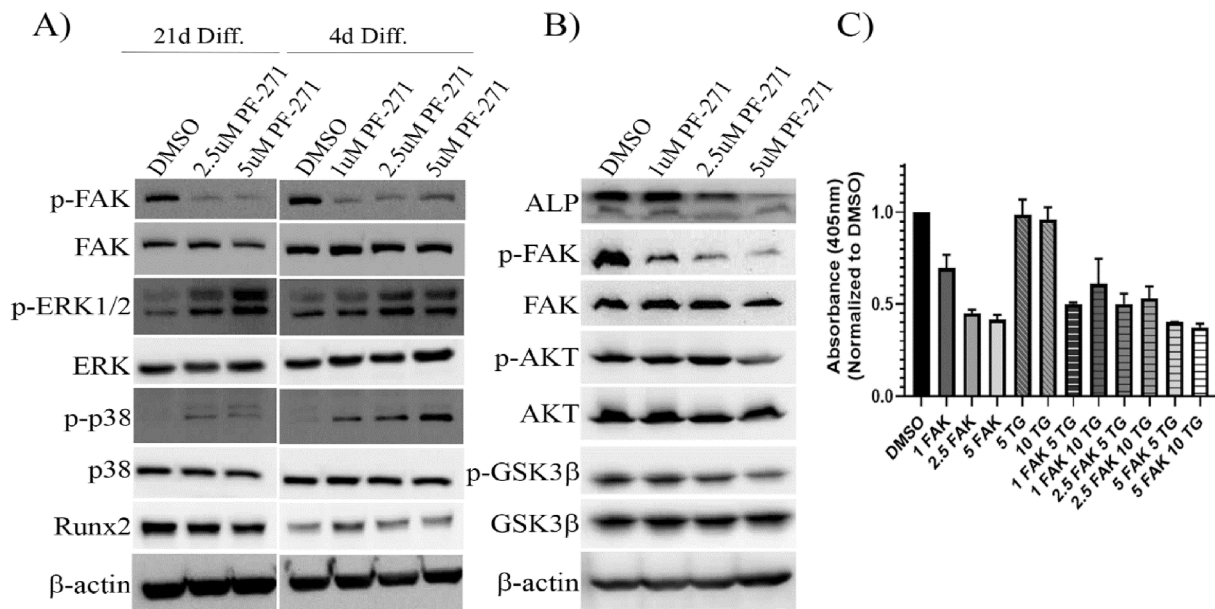


Fig. 6. Treatment of Differentiated MC3T3-E1 cells with PF-562,271 leads to decreased levels of active AKT, inactive GSK3 β and ALP, but inhibition of active GSK3 β does not restore PF-562,271 suppressed mineralization. (A) MC3T3-E1 cells were differentiated for 21 days as described in the Methods and were then treated with either DMSO as a vehicle control or various concentrations of PF-562,271 starting on day 4 or 21 of differentiation and were treated for an additional 3 and 6 days respectively at which time cellular protein lysates were generated. Samples were assessed for levels of various proteins as indicated with assessment of β -actin as a control for equivalent protein loading. (B) MC3T3-E1 cells were differentiated for 21 days as described in the Methods and were then treated with either DMSO as a vehicle control or various concentrations of PF-562,271 starting on day 21 of differentiation for an additional 6 days at which time cellular protein lysates were generated. Protein samples were then assessed for various forms of phospho or total proteins with assessment of β -actin as a control for equivalent protein loading. (C) MC3T3-E1 cells were differentiated for 21 days as described in the Methods and were then treated with either DMSO as a vehicle control or various concentrations of PF-562-271 (FAK) alone or in combination with 5 μ M or 10 μ M Tideglusib (TG) for an additional 6 days. Cells were then stained for alizarin red and dye extracted to measure absorbance as described in the Methods. Graphs represent mean and standard error of duplicate wells in each of three independent biological replicates.

also induced increased levels of active phospho-(Thr180/Tyr182) p38 at least at the earlier time points (Fig. 6A, Supplementary Table S3) suggesting it should promote increased Runx2 activity and ALP expression which we did not observe. As such, we speculated if ALP expression was decreased due to impaired Runx2 activity, then ERK1/2 and p38 independent mechanisms must be responsible. Another possible candidate was GSK3 β as it has previously been shown to inhibit ALP expression via its ability to phosphorylate Runx2 at S275, thereby inhibiting the transcriptional activity of Runx2 [41]. We thus tested levels of expression of inactive (i.e. phosphorylated) GSK3 β by western blot analysis of MC3T3-E1 cells exposed to 7 days of PF-562,271 treatment following a 21-day period of differentiation. We found that PF-562,271 treatment led to a dose-dependent decrease in inactive GSK3 β levels as measured by phosphorylation at S9 [42], while total GSK3 β levels remained unchanged (Fig. 6B, densitometry in Supplementary Table S3). This was concomitant with decreased phospho-Akt and ALP protein levels following PF-562,271 treatment (Fig. 6B, Supplementary Table S3). Decreased active Akt is correlated with decreases in phospho-S9-GSK3 β as active Akt has been shown to inhibit GSK3 β activity via this phosphorylation mechanism [43]. This suggests that treatment with PF-562,271 results in increased levels of active GSK3 β protein, which would in turn phosphorylate Runx2 to inhibit its transcriptional activity thereby leading to reduced ALP expression. We thus investigated whether inhibition of GSK3 β activity could restore MC3T3-E1 mineralization in the presence of PF-562,271. After 21 days of differentiation, MC3T3-E1 cells were exposed to vehicle control, PF-562,271, the irreversible GSK3 β inhibitor Tideglusib (TG; a non-ATP competitive GSK3 β inhibitor) or PF-562,271 and TG in combination for 7 days. Mineralization was then assessed by Alizarin Red staining and subsequent quantification. Simultaneous co-administration of TG did not overcome the inhibitory effects of PF-562,271 on MC3T3-E1 mineralization although some non-significant trends for increased mineralization were observed when TG was given together with lower doses of PF-562,271

(Fig. 6C, ~11–17 % increase in mineralization with addition of TG and treatment with 2.5 μ M PF-562,271). Use of alternative GSK3 β inhibitors TWS119 or SB216763 also failed to restore MC3T3-E1 mineralization in similar assays (data not shown).

3.5. FAK TKIs alter phenotype of differentiated MC3T3-E1 cells via reduced levels of osterix.

Given the inability to restore MC3T3-E1 mineralization in the presence of PF-562,271 using the approaches we employed, we speculated that perhaps treatment with PF-562,271 had irreversible effects on differentiated MC3T3-E1 cells. We first confirmed that treated MC3T3-E1 did not undergo apoptosis following treatment with PF-562,271 by assessing expression of cleaved PARP and cleaved caspase-3 by western blot. No significant increase of these apoptotic markers was observed following PF-562,271 treatment (Fig. 7A), suggesting treated MC3T3-E1 remain viable after the 28-day differentiation and drug treatment protocol. SA- β -gal staining was also performed to assess whether senescence was induced in PF-562,271 treated MC3T3-E1 cells, however, we did not observe any significant differences in levels of SA- β -gal regardless of treatment (Fig. 7B). However, we noticed that PF-562,271 treated differentiated cells appeared larger, rounder and overall has less of a typical mesenchymal phenotype than control treated cells (Fig. 7B). We thus wondered whether PF-562,271 blocked further osteoblast differentiation or induced de-differentiation to a less mature stage thereby preventing mineralization, or whether PF-562,271 could promote further differentiation of mature osteoblasts into osteocytes, with the reduced ALP expression observed in our assay system supporting the latter possibility. We therefore tested the levels of mRNA and protein expression of the osteocyte marker sclerostin in 28 day differentiated and drug treated MC3T3-E1 cells, however no significant differences in sclerostin levels following drug treatment were observed (data not shown) suggesting cells were not induced to become osteocytes.

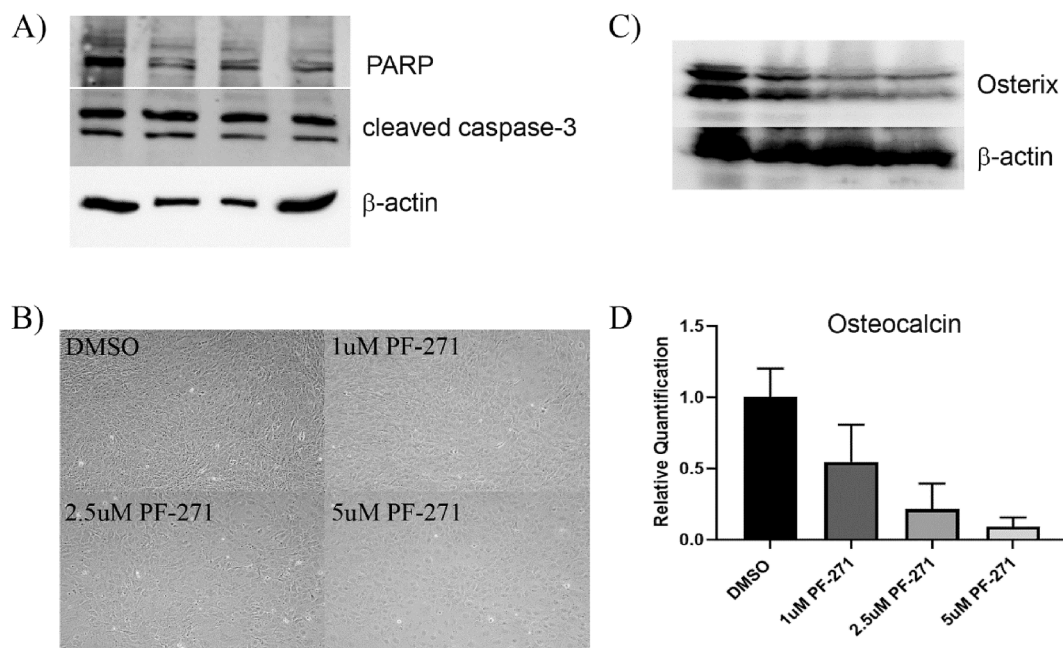


Fig. 7. Treatment of Differentiated MC3T3-E1 cells with PF-562,271 does not induce apoptosis or senescence however may block osteoblast maturation through inhibition of osterix and osteocalcin. (A) MC3T3-E1 cells were differentiated for 21 days as described in the Methods and were then treated with either DMSO as a vehicle control or various concentrations of PF-562,271 (PF271) for an additional 6 days at which time cellular protein lysates were generated. Levels of PARP and cleaved caspase-3 were assessed along with β -actin levels as a control for equivalent protein loading. (B) MC3T3-E1 cells were differentiated for 4 days then treated with DMSO or various concentrations of PF-562,271 for an additional 3 days at which time they were assessed for senescence using SA- β -gal detection and imaged as described in the Methods. (C) Cells from (A) were also assessed for levels of osterix by western blot, with assessment of β -actin levels as a control for equivalent protein loading. (D) MC3T3-E1 cells were differentiated for 21 days as described in the Methods and were then treated with either DMSO as a vehicle control or various concentrations of PF-562,271 for an additional 6 days at which time RNA was extracted and subjected to qRT-PCR for levels of osteocalcin. Graph represents mean delta-delta CT and associated standard error expressed as relative quantification normalized to DMSO controls and levels of β -actin in triplicate technical replicates for $n = 3$ biological replicates.

Although our initial results assessing levels of mRNA for osteoblast lineage transcription factors Runx2 and osterix suggested they were not altered at the mRNA level by treatment with PF-562,271 given at D21, we decided to confirm these findings at the protein level. As our data suggested there were no differences in total Runx2 (Fig. 6A), but perhaps altered transcriptional activity, we focused our examination on the other main transcription factor that regulates osteoblast differentiation, osterix. Interestingly, the protein stability of osterix has been shown to be regulated by Akt [44]. Since we observed decreased active Akt following treatment with PF-562,271 we speculated that osterix protein levels may be reduced by drug treatment leading to the decreased ALP levels and lack of mineralization in our assay system. We thus assessed levels of osterix in 28-day differentiated and drug treated (21 days differentiation media and 7 additional days of PF-562,271 treatment) MC3T3-E1 cells by western blot. As suspected, osterix protein levels showed dose-dependent decreases following treatment with PF-562,271 (Fig. 7C). We further confirmed at the mRNA level that PF-562,271 also resulted in dose-dependent decreased levels of the osteoblast marker osteocalcin (Fig. 7D), suggesting there are reduced levels of mature osteoblasts present following treatment. Thus, our data suggest that inhibition of FAK impairs Akt activity leading to reduced protein levels of osterix which in turn prevent sustained differentiation of osteoblasts and their ability to mineralize.

4. Discussion

4.1. Effects of FAK-TKI on early MC3T3-E1 differentiation.

Treating MC3T3-E1 cells with PF-562,271 starting at either D4 or D10 post addition of differentiation media, resulted in dose-dependent decreases in overall ALP staining and the percentage of ALP positive

cells (Fig. 1). This was also concomitant with a decrease in viable cell number following drug treatment with higher doses, however this did not appear to be a result of increased apoptosis since we did not see significant increases in levels of cleaved PARP or cleaved caspase-3 (Fig. 1). We speculate that at these earlier time points, FAK inhibition likely blocks MC3T3-E1 differentiation by downregulating levels of Runx2 and Osterix, since we have evidence their mRNA levels are dose-dependently reduced by treatment with PF-562,271 (Supplementary Fig. S2). Our findings are similar to those observed following depletion of FAK in MC3T3-E1 cells using stably expressed anti-sense mRNA to FAK whereby the authors observed a failure to differentiate concomitant with reduced ALP and Runx2 expression [26]. The ability of PF-562,271 to impair Runx2 mRNA expression at these early time points also likely contributes to the reduced number of viable cells we observed with higher doses of PF-562,271 as Runx2 has also been shown to promote osteoblast precursor proliferation via its ability to regulate fibroblast growth factor receptors 2 and 3 in osteoblast progenitor cells in vivo [45].

4.2. FAK TKI-mediated suppression of osteoblast mineralization.

Our findings suggest that treatment with the FAK inhibitor PF-562,271 potentially blocks osteoblast mineralization which has implications for restoration of normal bone homeostasis in patients treated with agents targeting FAK. Our findings are similar to those previously published using anti-sense mediated targeting of FAK in MC3T3-E1 cells, where FAK inhibition was associated with reduced ALP activity, osteocalcin expression and mineralization [26]. FAK inhibition using siRNA mediated interference was also shown to reduce ALP, osteocalcin and OPG in urine derived stem cells induced to differentiate into osteoblasts [46]. However, in this paper, the authors showed that BMP-2 mediated

osteoblast differentiation resulted in activation of FAK downstream of BMP-2 stimulation [46], and its inhibition using siRNA interference targeting FAK impaired BMP-2 induced osteoblastogenesis and mineralization. These findings could explain why we observed no restoration of mineralization upon inhibition of BMP-2 mediated signaling using LDN193189 (Fig. 4), as FAK is downstream of BMP-2 signaling and would remain impaired by concurrently administered PF-562,271 thereby leading to continued inhibition of mineralization. It also remains possible that despite upregulated BMP-2 mRNA levels at all time points examined, BMP-2 cellular protein levels are either not increased in response to PF-562,271 treatment or are not high enough to be detected by western blot. As BMP-2 is a secreted protein it is possible that elevated levels could be in cell conditioned supernatants, however we did not examine this as the differences we observed in mineralization following FAK inhibitor treatment could affect reliable measurement of secreted BMP-2 since it is known to bind to mineralized bone matrix [47].

4.3. FAK TKI treatment leads to decreased p53 levels but preventing p53 degradation does not restore mineralization defects induced by FAK TKI.

It has been reported that treatment of cells with PF-562,271 leads to accumulation of FAK in the cell nucleus as binding of the drug to the kinase domain of FAK keeps it in a 'closed' conformation which blocks access to its nuclear export signal [48]. It has also been shown that nuclear FAK leads to Mdm2 stabilization and degradation of its target p53 thereby promoting cellular growth and survival [34]. The importance of Mdm2 in osteogenesis has been previously described using osteoblast lineage directed genetic knockout of floxed Mdm2 following expression of Col3.6-Cre in transgenic mice. The authors showed that osteoblast lineage conditional Mdm2 $-/-$ mice died at birth with multiple skeletal defects [33]. They could further show that osteogenic precursor cells isolated from these animals had impaired ability to mineralize *in vitro* assays which was concomitant with increased levels of active p53 and reduced levels of Runx2 protein [33]. We confirmed the finding that treatment of MC3T3-E1 cells with FAK TKI did lead to decreased levels of p53 as previously described suggesting PF-562,271 stabilizes Mdm2 as proposed, however we did not see increased mineralization as a result. Although we speculated Mdm2 may degrade other proteins important for mineralization, our attempts to restore mineralization by more selectively blocking Mdm2 stabilization in our assay system were unsuccessful. We speculate this is due to p53-independent barriers to osteoblast maturation as discussed below, or perhaps due to suppression of other osteoblastogenic factors upon increased p53 levels following Mdm2 inhibition, given p53 has been shown to suppress Runx2 and osterix levels [49]. Despite Mdm2-induced decreases in p53 following treatment with PF-562,271, we did not see increases in either Runx2 (Fig. 6) or osterix (Fig. 7) protein levels under these conditions as would be expected with loss of p53. This data further supports our contention that additional mechanisms downstream of p53 are predominantly responsible for the observed block in mineralization induced by PF-562,271. Despite this, it is important to highlight that pharmacological inhibition of FAK did result in increased Mdm2 activity as evidenced by decreased p53 protein levels in MC3T3-E1 cells in our assays. This should be taken into consideration as it remains possible that despite our attempts to alter activity of known downstream FAK TKI-sensitive pathways involved in osteoblast differentiation and mineralization, the blocking of these pathways was done in isolation, and thus elevated Mdm2 activity would remain and could contribute to the inhibition of these processes in our assay systems via undetermined mechanisms.

4.4. FAK TKI treatment of MC3T3-E1 cells leads to increased GSK3 β activity which can impair the transcriptional activity of Runx2.

We originally thought that FAK activity was required upstream of important factors regulating osteoblastogenesis and mineralization,

such as Runx2, given that FAK was previously shown to be activated in mesenchymal stromal cells induced to differentiate into osteoblasts prior to observed induction of Runx2 levels in this model system [50]. However, despite observing inhibition at early time points, we did not see any decrease in mRNA levels of either Runx2 or osterix following treatment of 21 day differentiated MC3T3-E1 cells with PF-562,271 (Fig. 3). We thus speculated that FAK controlled the activity as opposed to the expression of these downstream transcription factors in differentiated cells. We hypothesized that due to the PF-562,271-mediated reduction of active Akt that we observed, it was possible that Akt inhibition of GSK3 β activity via its ability to phosphorylate Ser9 [43] would be reduced, leading to increased GSK3 β activity which in turn inhibited Runx2 activity [41]. Although we did not formally demonstrate reduced Runx2 activity, our hypothesis is supported by our results showing decreased phospho-S9-GSK3 β concomitant with decreased phospho-S473-Akt and decreased expression of osteocalcin in response to treatment with PF-562,271 (Figs. 6 and 7). Although we attempted to restore mineralization by blocking GSK3 β activity using specific inhibitors but did not observe increased osteoblast mineralization in the presence of PF-562,271, it should be noted that treatment with the GSK3 β inhibitors alone at the doses used (5-10 μ M) did not promote mineralization either in our assay system as we would have predicted. Although not significant, there is a trend that Tideglusib increased mineralization in the presence of the lower 2.5 μ M PF-562,271 dose and the use of higher doses of Tideglusib may restore this further. We restricted our assessment to these lower drug concentrations however, as although Tideglusib effectively restores phosphorylation of GSK3 β at Ser9 at 15 μ M, it can also induce apoptosis of cells at this concentration [51]. Thus, it remains possible that this mechanism of osteoblast mineralization may play an important role in our studies, but we are unable to formally demonstrate this effectively without the additional caveat of inducing apoptosis of osteoblasts in the process.

4.5. FAK TKI treatment of MC3T3-E1 cells leads to reduced protein levels of osterix in part mediated by suppression of Akt activity

Other possible factors which may contribute to our observed results could be the effect of FAK inhibitors on Akt activity. Although the blots shown in Fig. 6 show moderate decreases in phospho-S473 Akt at 5 μ M doses of PF-562,271, it should be noted that protein extracts were derived 72–96 h post addition of PF-562,271 at which point the FAK inhibitor may be depleted and Akt activity may be partially restored. Furthermore, densitometry of levels of phospho-S473 Akt/total Akt/GAPDH in $n = 3$ independently generated experimental samples showed a 70 % reduction in phospho-S473 Akt levels following treatment with 5 μ M PF-562,271 (Supplementary Table S3). We have also previously observed consistent potent inhibition of Akt by PF-562,271 at earlier time points post drug addition in other cell types [29] and in 4 day differentiated MC3T3-E1 cells 48 h post PF-562,271 treatment (Supplementary Figure S3). The ability of various FAK TKIs including PF-562,271 to reduce phospho-S473 Akt levels has also been established by others [22,52–54], and it is well known that Akt is activated downstream of FAK [55–58]. It has been shown that Akt activity is required for osteoblast differentiation, ALP expression and mineralization, and expression of dominant negative Akt additionally blocked mineralization when added at late time points in the process [59]. Interestingly, in the paper by Mukherjee and Rotwein [59], expression of dominant negative Akt appeared to inhibit mRNA expression of Runx2, osterix and osteocalcin concomitant with reduced mineralization [59]. In our case, treatment with FAK inhibitor in 21 day differentiated MC3T3-E1 cells did not seem to alter the mRNA levels of Runx2 or osterix, however the protein levels of osterix and phosphorylation status of Runx2 were altered. As these authors also demonstrated that Akt activity is required throughout the differentiation and mineralization process, we speculate that PF-562,271 added during the process of pre-osteoblast to osteoblast maturation and mineralization stage beginning at day 21 sufficiently

impairs Akt activity resulting in decreased osterix, osteocalcin and ALP levels translating into decreased mineralization. The reduced osteocalcin expression further suggests that perhaps cells remain in a pre-osteoblast stage and are not fully matured which is also supported by their altered phenotypic appearance (Fig. 7) following treatment with PF-562,271. The dominant role of active Akt in osteoblast mineralization is supported by the findings of Suzuki *et al.* [60], who showed that expression of constitutively active Akt resulted in enhanced mineralization by differentiated MC3T3-E1 cells, even during concurrent treatment with TGF β which would normally suppress MC3T3-E1 mineralization in their assay system. Moreover, they also observed that dominant negative Akt expression blocked osteocalcin expression [60], similar to what we have observed following PF-562,271 treatment (Fig. 7). The ability of PF-562,271 to inhibit Akt-mediated osterix expression could also in part explain why our attempts to restore mineralization by blocking GSK3 β -induced inhibition of Runx2 activity were not successful. While we saw no change in mRNA levels of osterix following treatment of 21 day differentiated MC3T3-E1 cells with PF-562,271, protein levels were reduced (Fig. 7), which we propose is mediated by the lack of active Akt, as Akt has been shown to regulate osterix activity in part by stabilizing it at the protein level [44]. Overall our data support a mechanism whereby PF-562,271 mediated suppression of FAK-induced Akt activation reduces osterix protein levels resulting in the impairment of osteoblast maturation and mineralization.

Our findings suggest that FAK plays an integral role in osteoblast differentiation and mineralization including possible regulation of important factors such as Mdm2, GSK3 β , Runx2, Akt and osterix. We have demonstrated that in addition to its ability to regulate osteoclast activity as previously reported, FAK TKIs also potently suppress osteoblastogenesis and mineralization activities. Thus, while their use in disorders resulting from excessive bone growth may be desirable, their use as a therapy to block bone degradation mediated primarily by osteoclasts would additionally be associated with the prevention of bone growth and restoration by osteoblasts which may be undesirable.

CRedit authorship contribution statement

Scott A. Gunn: Conceptualization, Data curation, Methodology, Formal analysis, Writing – review & editing. **Lauren M. Kreps:** Data curation, Formal analysis, Writing – review & editing. **Huijun Zhao:** Data curation, Formal analysis, Writing – review & editing. **Katelyn Landon:** Conceptualization, Data curation, Methodology, Formal analysis, Writing – review & editing. **Jacob S. Ilacqua:** Data curation, Formal analysis, Writing – review & editing. **Christina L. Addison:** Conceptualization, Data curation, Formal analysis, Funding acquisition, Methodology, Supervision, Validation, Writing – original draft, Writing – review & editing.

Declaration of Competing Interest

The authors declare that they have no known competing financial interests or personal relationships that could have appeared to influence the work reported in this paper.

Acknowledgements

This work was supported by funding awarded to CLA from the Canadian Cancer Society (BC-RG-16 - 2016 (319330)). The funding agency had no role in the study design, collection, analysis and interpretation of data, or the writing of this manuscript and decision to submit the article for publication

Appendix A. Supplementary data

Supplementary data to this article can be found online at <https://doi.org/10.1016/j.jbo.2022.100432>.

References

- [1] H. Kennecke, R. Yerushalmi, R. Woods, M.C. Cheang, D. Voduc, C.H. Speers, T. O. Nielsen, K. Gelmon, Metastatic behavior of breast cancer subtypes, *J. Clin. Oncol.* 28 (20) (2010) 3271–3277.
- [2] G.R. Mundy, Mechanisms of bone metastasis, *Cancer* 80 (8 Suppl) (1997) 1546–1556.
- [3] M. Luo, J.L. Guan, Focal adhesion kinase: a prominent determinant in breast cancer initiation, progression and metastasis, *Cancer Lett.* 289 (2) (2010) 127–139.
- [4] P.P. Provenzano, P.J. Keely, The role of focal adhesion kinase in tumor initiation and progression, *Cell Adhes. Migr.* 3 (4) (2009) 347–350.
- [5] H. Lahlou, V. Sanguin-Gendreau, D. Zuo, R.D. Cardiff, G.W. McLean, M.C. Frame, W.J. Muller, Mammary epithelial-specific disruption of the focal adhesion kinase blocks mammary tumor progression, *PNAS* 104 (51) (2007) 20302–20307.
- [6] R. Stanzione, A. Picascia, P. Chieffi, C. Imbimbo, A. Palmieri, V. Mirone, S. Staibano, R. Franco, G. De Rosa, J. Schlessinger, D. Tramontano, Variations of proline-rich kinase Pyk2 expression correlate with prostate cancer progression, *Lab. Invest.* 81 (1) (2001) 51–59.
- [7] L. Ding, X. Sun, Y. You, N. Liu, Z. Fu, Expression of focal adhesion kinase and phosphorylated focal adhesion kinase in human gliomas is associated with unfavorable overall survival, *Transl. Res.* 156 (1) (2010) 45–52.
- [8] J.H. Park, B.L. Lee, J. Yoon, J. Kim, M.A. Kim, H.K. Yang, W.H. Kim, Focal adhesion kinase (FAK) gene amplification and its clinical implications in gastric cancer, *Hum. Pathol.* 41 (12) (2010) 1664–1673.
- [9] J.C. de Vicente, P. Rosado, P. Lequerica-Fernandez, E. Allonca, L. Villallain, G. Hernandez-Vallejo, Focal adhesion kinase overexpression: correlation with lymph node metastasis and shorter survival in oral squamous cell carcinoma, *Head Neck* 35 (6) (2013) 826–830.
- [10] H.F. Ji, D. Pang, S.B. Fu, Y. Jin, L. Yao, J.P. Qi, J. Bai, Overexpression of focal adhesion kinase correlates with increased lymph node metastasis and poor prognosis in non-small-cell lung cancer, *J. Cancer Res. Clin. Oncol.* 139 (3) (2013) 429–435.
- [11] S. Nakayamada, Y. Okada, K. Saito, M. Tamura, Y. Tanaka, Beta1 integrin/focal adhesion kinase-mediated signaling induces intercellular adhesion molecule 1 and receptor activator of nuclear factor kappaB ligand on osteoblasts and osteoclast maturation, *J. Biol. Chem.* 278 (46) (2003) 45368–45374.
- [12] Y. Matsumoto, K. Tanaka, G. Hirata, M. Hanada, S. Matsuda, T. Shuto, Y. Iwamoto, Possible involvement of the vascular endothelial growth factor-Flt-1-focal adhesion kinase pathway in chemotaxis and the cell proliferation of osteoclast precursor cells in arthritic joints, *J. Immunol.* 168 (11) (2002) 5824–5831.
- [13] W.C. Xiong, X. Feng, PYK2 and FAK in osteoclasts, *Front Biosci* 8 (2003) d1219–d1226.
- [14] J.B. Kim, P. Leucht, C.A. Luppen, Y.J. Park, H.E. Beggs, C.H. Damsky, J.A. Helms, Reconciling the roles of FAK in osteoblast differentiation, osteoclast remodeling, and bone regeneration, *Bone* 41 (1) (2007) 39–51.
- [15] T. Sen, A. Dutta, G. Maity, A. Chatterjee, Fibronectin induces matrix metalloproteinase-9 (MMP-9) in human laryngeal carcinoma cells by involving multiple signaling pathways, *Biochimie* 92 (10) (2010) 1422–1434.
- [16] G. Maity, S. Fahreen, A. Banerji, P. Roy Choudhury, T. Sen, A. Dutta, A. Chatterjee, Fibronectin–integrin mediated signaling in human cervical cancer cells (SiHa), *Mol. Cell. Biochem.* 336 (1–2) (2010) 65–74.
- [17] W.G. Roberts, E. Ung, P. Whalen, B. Cooper, C. Hulford, C. Autry, D. Richter, E. Emerson, J. Lin, J. Kath, K. Coleman, L. Yao, L. Martinez-Alsina, M. Lorenzen, M. Berliner, M. Luzzio, N. Patel, E. Schmitt, S. LaGreca, J. Jani, M. Wessel, E. Marr, M. Griffor, F. Vajdos, Antitumor activity and pharmacology of a selective focal adhesion kinase inhibitor, PF-562,271, *Cancer Res.* 68 (6) (2008) 1935–1944.
- [18] V.M. Golubovskaya, C. Nyberg, M. Zheng, F. Kweh, A. Magis, D. Ostrov, W. G. Cance, A small molecule inhibitor, 1,2,4,5-benzenetetraamine tetrahydrochloride, targeting the y397 site of focal adhesion kinase decreases tumor growth, *J. Med. Chem.* 51 (23) (2008) 7405–7416.
- [19] A. Mousson, E. Sick, P. Carl, D. Dujardin, J. De Mey, P. Rondé, Targeting focal adhesion kinase using inhibitors of protein-protein interactions, *Cancers* 10 (9) (2018) 278.
- [20] S. Wang, M.D. Basson, Akt directly regulates focal adhesion kinase through association and serine phosphorylation: implication for pressure-induced colon cancer metastasis, *Am. J. Physiol. Cell Physiol.* 300 (3) (2011) C657–C670.
- [21] H. Fan, X. Zhao, S. Sun, M. Luo, J.L. Guan, Function of focal adhesion kinase scaffolding to mediate endophilin A2 phosphorylation promotes epithelial-mesenchymal transition and mammary cancer stem cell activities in vivo, *J. Biol. Chem.* 288 (5) (2013) 3322–3333.
- [22] C. Hu, X. Chen, J. Wen, L. Gong, Z. Liu, J. Wang, J. Liang, F. Hu, Q. Zhou, L. Wei, Y. Shen, W. Zhang, Antitumor effect of focal adhesion kinase inhibitor PF562271 against human osteosarcoma in vitro and in vivo, *Cancer Sci.* 108 (7) (2017) 1347–1356.
- [23] N. Kurio, T. Shimo, T. Fukazawa, M. Takaoka, T. Okui, N.M. Hassan, T. Honami, S. Hatakeyama, M. Ikeda, Y. Naomoto, A. Sasaki, Anti-tumor effect in human breast cancer by TAE226, a dual inhibitor for FAK and IGF-IR in vitro and in vivo, *Exp. Cell Res.* 317 (8) (2011) 1134–1146.
- [24] C.M. Bagi, G.W. Roberts, C.J. Andresen, Dual focal adhesion kinase/Pyk2 inhibitor has positive effects on bone tumors: implications for bone metastases, *Cancer* 112 (10) (2008) 2313–2321.
- [25] Y. Takeuchi, M. Suzawa, T. Kikuchi, E. Nishida, T. Fujita, T. Matsumoto, Differentiation and transforming growth factor-beta receptor down-regulation by collagen-alpha2beta1 integrin interaction is mediated by focal adhesion kinase and its downstream signals in murine osteoblastic cells, *J. Biol. Chem.* 272 (46) (1997) 29309–29316.

- [26] Y. Tamura, Y. Takeuchi, M. Suzawa, S. Fukumoto, M. Kato, K. Miyazono, T. Fujita, Focal adhesion kinase activity is required for bone morphogenetic protein-Smad1 signaling and osteoblastic differentiation in murine MC3T3-E1 cells, *J. Bone Mineral Res.* 16 (10) (2001) 1772–1779.
- [27] F. Debacq-Chainiaux, J.D. Erusalimsky, J. Campisi, O. Toussaint, Protocols to detect senescence-associated beta-galactosidase (SA-beta-gal) activity, a biomarker of senescent cells in culture and in vivo, *Nat. Protoc.* 4 (12) (2009) 1798–1806.
- [28] M.A. Cabrita, L.M. Jones, J.L. Quizi, L.A. Sabourin, B.C. McKay, C.L. Addison, Focal adhesion kinase inhibitors are potent anti-angiogenic agents, *Mol. Oncol.* 5 (6) (2011) 517–526.
- [29] G.A. Howe, B. Xiao, H. Zhao, K.N. Al-Zahrani, M.S. Hasim, J. Villeneuve, H. S. Sekhon, G.D. Goss, L.A. Sabourin, J. Dimitrakopoulos, C.L. Addison, J.J.W. Chen, Focal adhesion kinase inhibitors in combination with erlotinib demonstrate enhanced anti-tumor activity in non-small cell lung cancer, *PLoS ONE* 11 (3) (2016) e0150567.
- [30] P.P. Eleniste, V. Patel, S. Positong, O. Zero, H. Largura, Y.H. Cheng, E.R. Himes, M. Hamilton, J. Baughman, M.A. Kacena, A. Bruzzaniti, Pyk2 and megakaryocytes regulate osteoblast differentiation and migration via distinct and overlapping mechanisms, *J. Cell. Biochem.* 117 (6) (2016) 1396–1406.
- [31] L. Buckbinder, D.T. Crawford, H. Qi, H.Z. Ke, L.M. Olson, K.R. Long, P.C. Bonnette, A.P. Baumann, J.E. Hambor, W.A. Grasser 3rd, L.C. Pan, T.A. Owen, M.J. Luzzio, C. A. Hulford, D.F. Gebhard, V.M. Paralkar, H.A. Simmons, J.C. Kath, W.G. Roberts, S. L. Smock, A. Guzman-Perez, T.A. Brown, M. Li, Proline-rich tyrosine kinase 2 regulates osteoprogenitor cells and bone formation, and offers an anabolic treatment approach for osteoporosis, *PNAS* 104 (25) (2007) 10619–10624.
- [32] K. Fujita, S. Janz, Attenuation of WNT signaling by DKK-1 and -2 regulates BMP2-induced osteoblast differentiation and expression of OPG, RANKL and M-CSF, *Mol. Cancer* 6 (2007) 71.
- [33] C.J. Lengner, H.A. Steinman, J. Gagnon, T.W. Smith, J.E. Henderson, B.E. Cream, G.S. Stein, J.B. Lian, S.N. Jones, Osteoblast differentiation and skeletal development are regulated by Mdm2-p53 signaling, *J. Cell Biol.* 172 (6) (2006) 909–921.
- [34] S.T. Lim, X.L. Chen, Y. Lim, D.A. Hanson, T.T. Vo, K. Howerton, N. Larocque, S. J. Fisher, D.D. Schlaepfer, D. Ilic, Nuclear FAK promotes cell proliferation and survival through FERM-enhanced p53 degradation, *Mol. Cell* 29 (1) (2008) 9–22.
- [35] G. Rawadi, B. Vayssières, F. Dunn, R. Baron, S. Roman-Roman, BMP-2 controls alkaline phosphatase expression and osteoblast mineralization by a Wnt autocrine loop, *J. Bone Mineral Res.* 18 (10) (2003) 1842–1853.
- [36] J.L. Millan, M.P. Whyte, Alkaline phosphatase and hypophosphatasia, *Calcif. Tissue Int.* 98 (4) (2016) 398–416.
- [37] C. Halling Linder, B. Ek-Rylander, M. Krumpel, M. Norgard, S. Narisawa, J. L. Millan, G. Andersson, P. Magnusson, Bone alkaline phosphatase and tartrate-resistant acid phosphatase: potential co-regulators of bone mineralization, *Calcif. Tissue Int.* 101 (1) (2017) 92–101.
- [38] C.G. Bellows, J.E. Aubin, J.N. Heersche, Initiation and progression of mineralization of bone nodules formed in vitro: the role of alkaline phosphatase and organic phosphate, *Bone Mineral* 14 (1) (1991) 27–40.
- [39] S. Gallea, F. Lallemand, A. Atfi, G. Rawadi, V. Ramez, S. Spinella-Jaegle, S. Kawai, C. Faucheu, L. Huet, R. Baron, S. Roman-Roman, Activation of mitogen-activated protein kinase cascades is involved in regulation of bone morphogenetic protein-2-induced osteoblast differentiation in pluripotent C2C12 cells, *Bone* 28 (5) (2001) 491–498.
- [40] C. Ge, Q. Yang, G. Zhao, H. Yu, K.L. Kirkwood, R.T. Franceschi, Interactions between extracellular signal-regulated kinase 1/2 and p38 MAP kinase pathways in the control of RUNX2 phosphorylation and transcriptional activity, *J. Bone Mineral Res.* 27 (3) (2012) 538–551.
- [41] F. Kugimiya, H. Kawaguchi, S. Ohba, N. Kawamura, M. Hirata, H. Chikuda, Y. Azuma, J.R. Woodgett, K. Nakamura, U.I. Chung, GSK-3beta controls osteogenesis through regulating Runx2 activity, *PLoS ONE* 2 (9) (2007) e837.
- [42] C. Sutherland, I.A. Leighton, P. Cohen, Inactivation of glycogen synthase kinase-3 beta by phosphorylation: new kinase connections in insulin and growth-factor signalling, *Biochem. J.* 296 (Pt 1) (1993) 15–19.
- [43] D.A. Cross, D.R. Alessi, P. Cohen, M. Andjelkovich, B.A. Hemmings, Inhibition of glycogen synthase kinase-3 by insulin mediated by protein kinase B, *Nature* 378 (6559) (1995) 785–789.
- [44] Y.H. Choi, H.M. Jeong, Y.H. Jin, H. Li, C.Y. Yeo, K.Y. Lee, Akt phosphorylates and regulates the osteogenic activity of Osterix, *Biochem. Biophys. Res. Commun.* 411 (3) (2011) 637–641.
- [45] T. Kawane, X. Qin, Q. Jiang, T. Miyazaki, H. Komori, C.A. Yoshida, V. Matsuura-Kawata, C. Sakane, Y. Matsuo, K. Nagai, T. Maeno, Y. Date, R. Nishimura, T. Komori, Runx2 is required for the proliferation of osteoblast progenitors and induces proliferation by regulating Fgfr2 and Fgfr3, *Sci. Rep.* 8 (1) (2018) 13551.
- [46] X. Sun, W. Zheng, C. Qian, Q. Wu, Y. Hao, G. Lu, Focal adhesion kinase promotes BMP2-induced osteogenic differentiation of human urinary stem cells via AMPK and Wnt signaling pathways, *J. Cell. Physiol.* 235 (5) (2020) 4954–4964.
- [47] M. Suzawa, Y. Takeuchi, S. Fukumoto, S. Kato, N. Ueno, K. Miyazono, T. Matsumoto, T. Fujita, Extracellular matrix-associated bone morphogenetic proteins are essential for differentiation of murine osteoblastic cells in vitro, *Endocrinology* 140 (5) (1999) 2125–2133.
- [48] S.T. Lim, N.L. Miller, X.L. Chen, I. Tancioni, C.T. Walsh, C. Lawson, S. Uryu, S. M. Weis, D.A. Cheres, D.D. Schlaepfer, Nuclear-localized focal adhesion kinase regulates inflammatory VCAM-1 expression, *J. Cell Biol.* 197 (7) (2012) 907–919.
- [49] A. Molchadsky, I. Shats, N. Goldfinger, M. Pevsner-Fischer, M. Olson, A. Rinon, E. Tzahor, G. Lozano, D. Zipori, R. Sarig, V. Rotter, T. Preiss, p53 plays a role in mesenchymal differentiation programs, in a cell fate dependent manner, *PLoS ONE* 3 (11) (2008) e3707.
- [50] R.M. Salasnyk, R.F. Klees, W.A. Williams, A. Boskey, G.E. Plopper, Focal adhesion kinase signaling pathways regulate the osteogenic differentiation of human mesenchymal stem cells, *Exp. Cell Res.* 313 (1) (2007) 22–37.
- [51] T.L. Mathuram, V. Ravikumar, L.M. Reece, S. Karthik, C.S. Sasikumar, K. M. Cherian, Tideglusib induces apoptosis in human neuroblastoma IMR32 cells, provoking sub-G0/G1 accumulation and ROS generation, *Environ. Toxicol. Pharmacol.* 46 (2016) 194–205.
- [52] H. Zhang, H. Shao, V.M. Golubovskaya, H. Chen, W. Cance, A.A. Adjei, G.K. Dy, Efficacy of focal adhesion kinase inhibition in non-small cell lung cancer with oncogenically activated MAPK pathways, *Br. J. Cancer* 115 (2) (2016) 203–211.
- [53] H. Moritake, Y. Saito, D. Sawa, N. Sameshima, A. Yamada, M. Kinoshita, S. Kamimura, T. Konomoto, H. Nuno, TAE226, a dual inhibitor of focal adhesion kinase and insulin-like growth factor-I receptor, is effective for Ewing sarcoma, *Cancer Med.* 8 (18) (2019) 7809–7821.
- [54] B.D. Crompton, A.L. Carlton, A.R. Thorne, A.L. Christie, J. Du, M.L. Calicchio, M. N. Rivera, M.D. Fleming, N.E. Kohl, A.L. Kung, K. Stegmaier, High-throughput tyrosine kinase activity profiling identifies FAK as a candidate therapeutic target in Ewing sarcoma, *Cancer Res.* 73 (9) (2013) 2873–2883.
- [55] H. Xia, R.S. Nho, J. Kahm, J. Kleidon, C.A. Henke, Focal adhesion kinase is upstream of phosphatidylinositol 3-kinase/Akt in regulating fibroblast survival in response to contraction of type I collagen matrices via a beta 1 integrin viability signaling pathway, *J. Biol. Chem.* 279 (31) (2004) 33024–33034.
- [56] Y. Chen, Z. Wang, P. Chang, L. Xiang, F. Pan, J. Li, J. Jiang, L. Zou, L. Yang, Z. Bian, H. Liang, The effect of focal adhesion kinase gene silencing on 5-fluorouracil chemosensitivity involves an Akt/NF-kappaB signaling pathway in colorectal carcinomas, *International journal of cancer, J. Internat. du Cancer* 127 (1) (2010) 195–206.
- [57] W. Xiong, J.T. Parsons, Induction of apoptosis after expression of PYK2, a tyrosine kinase structurally related to focal adhesion kinase, *J. Cell Biol.* 139 (2) (1997) 529–539.
- [58] B. Tavora, S. Batista, L.E. Reynolds, S. Jadjaja, S. Robinson, V. Kostourou, I. Hart, M. Fruttiger, M. Parsons, K.M. Hodivala-Dilke, Endothelial FAK is required for tumour angiogenesis, *EMBO Mol. Med.* 2 (12) (2010) 516–528.
- [59] A. Mukherjee, P. Rotwein, Akt promotes BMP2-mediated osteoblast differentiation and bone development, *J. Cell Sci.* 122 (Pt 5) (2009) 716–726.
- [60] E. Suzuki, H. Ochiai-Shino, H. Aoki, S. Onodera, A. Saito, T. Azuma, Akt activation is required for TGF-beta1-induced osteoblast differentiation of MC3T3-E1 pre-osteoblasts, *PLoS ONE* 9 (12) (2014) e112566.